flow distributions. This was due to both the high level of cell resolution allowed by the unstructured adaptive mesh and the robust performance of the shock capturing flux limiter.

Acknowledgment

The authors would like to acknowledge valuable discussions with K. Kailasanath, R. Ramamurti, and D. Book.

References

[1]Back, L. H., and Cuffel, R. F., "Detection of Oblique Shocks in a Conical Nozzle with a Circular-Arc Throat," *AIAA Journal,* Vol. 4, No. 12, 1966, pp. 2219-2221.

[2]Thornhill, D., and Ness, R., private communication, Lockheed Missile & Space Co., Palo Alto, CA, 1988-1989.

[3]Adamson, T. C., and Nichols, J. A., "On the Structure of Jets from Highly Underexpanded Nozzles into Still Air," *Journal of Aerospace Sciences,* Vol. 26, No. 1, 1959, pp. 16-24.

[4]Addy, A. L., Dutton, J. C., and Amatucci, V. A., "Nonuniform Nozzle Flow Effects on Base Pressure at Supersonic Flight Speeds," *AIAA Journal,* Vol. 24, No. 7, 1986, pp. 1209-1212.

[5]Serra, J., "Determination of Internal Gas Flows by a Transient Numerical Technique," *AIAA Journal,* Vol. 10, No. 5, 1972, pp. 603-611.

[6]Löhner, R., Baum, J. D., Loth, E., and Ramamurti, R., "A Finite Element Solver for Axisymmetric Compressible Flows," AIAA Paper 89-1794, Buffalo, NY, June, 1989.

[7]Löhner, R., Morgan, K., Peraire, J., and Vahdati, M., "Finite Element Flux Corrected Transport (FEM-FCT) for the Euler and Navier-Stokes Equations," *International Journal of Numerical Methods in Fluids,* Vol. 7, No. 10, 1987, pp. 1093-1109.

[8]Löhner, R., Morgan, K., and Zienkiewicz, O. C., "An Adaptive Finite Element Procedure for High Speed Flows," *Computer Methods in Applied Mechanics and Engineering,* Vol. 51, No. 1-3, 1985, pp. 441-465.

[9]Roe, P. L., "Error Estimates for Cell-Vertex Solvers of the Compressible Euler Equation," Institute for Computer Applications in Science and Engineering, Rept. 87-6, Langley, VA, 1987.

[10]Oran, E. S., and Boris, J. P., *Numerical Simulation of Reactive Flow,* Elsevier, New York, 1987.

[11]Loth, E. Baum, J. D., and Löhner, R., "Formation of Shocks Within Axisymmetric Flows," AIAA Paper 90-1655, Buffalo, NY, June 1990.

Turbulent Boundary-Layer Characteristics over a Flat-Plate/ Wedge Configuration at Mach 6

P. J. Disimile*
University of Cincinnati, Cincinnati, Ohio 45221
and
N. E. Scaggs†
Air Force Wright Research and Development Center, Wright-Patterson Air Force Base, Ohio 45433

Nomenclature

P_0 = stagnation pressure
P_t = local pitot pressure
P_s = static pressure
P_i = surface pressure at a given xy location
P_{ref} = undisturbed reference surface pressure acquired at $x = -6.469$ cm
Re = unit Reynolds number/meter
T_0 = stagnation temperature
T_t = local total temperature
T_s = static temperature
U = local mean velocity
U_{inf} = freestream velocity
x, y, z = streamwise, lateral (along the plate's width), and perpendicular to plate distance
δ = boundary-layer thickness
δ_T = thermal boundary-layer thickness (where T_t is 1% of the freestream)

Presented as Paper 90-3028 at the AIAA 8th Applied Aerodynamics Conference, Portland, OR, Aug. 20-22, 1990; received June 27, 1990; revision received Dec. 28, 1990; accepted for publication Dec. 28, 1990.

*Bradley Jones Associate Professor, Department of Aerospace Engineering. Member AIAA

†Technical Manager. Senior Member AIAA.

Introduction

A RECENT review of aerothermodynamic problems surrounding hypersonic flight and its associated research by Holden[1] demonstrates our present lack of predictive capability. Holden states that the intense research programs of the 1960s and early 1970s were superseded by hypersonic flow investigations that were limited to supporting specific missions such as the Space Shuttle, the Jovian entry vehicle, and ballistic re-entry vehicles. The results of this review vividly point out the scarcity of previous research encompassing turbulent boundary-layer separation and hypersonic flows.

Many earlier studies[2-7] on turbulent boundary-layer separation were preformed on smooth surfaces in supersonic-hypersonic flow regimes. These studies investigated incipient separation using compression corners to simulate flow over aerodynamic flaps or ailerons. Because high-speed flight vehicles employ various external control devices that can produce large areas of flow separation, a program was initiated to examine such effects.

Model and Experimental Facility

A smooth flat-plate/22 deg wedge configuration extending approximately 45.7 cm in streamwise length and 35.6 cm in lateral extent was machined to a no. 32 surface finish. A sharp 10-deg asymmetric leading edge was also machined into the model. Approximately 39.4 cm downstream from this leading edge was the intersection point of the instrumental wedge.

The model was then mounted downstream of a 30.5-cm open jet, high-Reynolds-number, Mach 6 blowdown wind tunnel. By adjusting the total pressure and stagnation temperature, unit Reynolds numbers ranging from approximately 33 to 98 $\times$ 10^6/m were obtained.

Model instrumentation consists of 46 surface pressure points and seven type-K (chromel/alumel) thermocouples. These ports were spaced streamwise in the x direction along the plate at its center ($y = 0$) and ± 9.5 mm off the center through the interaction region.

Boundary-Layer Characteristics

Distribution of both the total pressure and total temperature in the boundary layer were obtained using a pitot pressure probe and a Winkler-type temperature probe. To allow for high-resolution, near-wall total pressure measurements, the tip of the pressure probe was flattened resulting in an overall height of 0.51 mm. For the same reasoning, a miniature Winkler probe was fabricated measuring 1.52 mm in diameter. The recovery factor for this probe was determined to be 0.984 and the uncertainty in the temperature measurement is 2.2 K.

Traverses were performed at two streamwise locations, $x = -16.47$ and -5.52 cm upstream from the plate/wedge intersection point. A third traverse, perpendicular to the ramp surface at a distance along the surface equal to $+3.97$ cm downstream from the intersection point, was also performed. In addition, surface static pressure and wall temperatures were also recorded. From these measurements, the Mach number, velocity, and static temperature through the boundary layer were obtained.[8] Using numerical integration, the momentum thickness θ was computed for each unit Reynolds number and was found to be in good agreement when compared to the em-

pirical correlation of Roshko and Thomke[9] for a supersonic turbulent boundary layer. Although data was recorded at unit Reynolds numbers of 33 × 10^6/m, 66 × 10^6/m, and 98 × 10^6/m, because of room only the low-Reynolds-number case is presented.

The pitot pressure ratio on the ramp was observed to exhibit a completely different behavior than was obtained upstream of the ramp. A sizable peak in the pressure distribution obtained on the ramp was recorded. The magnitude of this peak is approximately three times greater than the P_t/P_0 ratio observed at locations upstream of the ramp (Fig. 1). This can be related to the local shock structure in the reattachment region. Utilizing inviscid oblique shock-wave theory, a shock angle of 31 deg is determined. Based on a freestream Mach number of 5.8, the pressure ratio was estimated to be 3.02. This value differed by < 3% from the experimentally determined pressure ratio of 3.1. Therefore, it appears that the effects of viscosity are indeed small.

The boundary-layer thickness δ, i.e., the position at which the local total pressure was observed to be $\leq 0.5\%$ of the freestream value, was used to indicate the boundary-layer edge. For the low-Reynolds-number case at $x = -5.517$ cm, δ was approximately 6.6 mm. Similarly δ_T was estimated to be 5.8 mm.

An examination of the surface pressure distribution in Fig. 2 indicates the two-dimensional nature of the flow. A comparison of surface pressures obtained at $y = 0$ and ± 0.95 cm indicate that excellent agreement exists over the center portion of the plate. In addition, only a 10% variation in P_s was observed over a 10.16-cm lateral spacing (approximately 15δ) in the same zone. Side fences were also added to the model and no notable difference in the surface pressure was observed. The separation point determined from schlieren photographs is estimated to extend approximately 2.54 mm upstream of the plate/wedge intersection point. Although difficult to measure, the extent of separation appeared to be identical for Reynold's numbers from 33 to 98 × 10^6/m.[10]

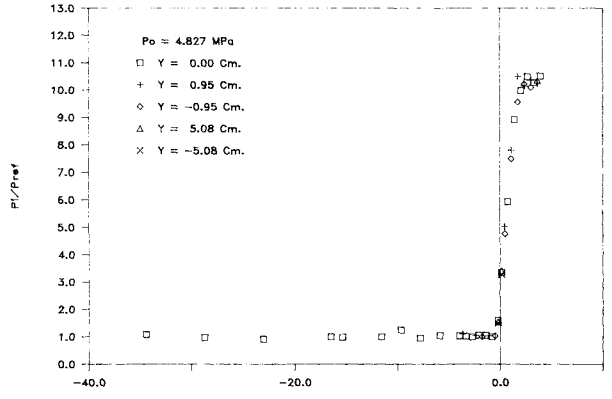

Fig. 1 Nondimensional total pressure ratio at $x = -16.47$ cm, $x = -5.52$ cm, and $x = +3.97$ cm.

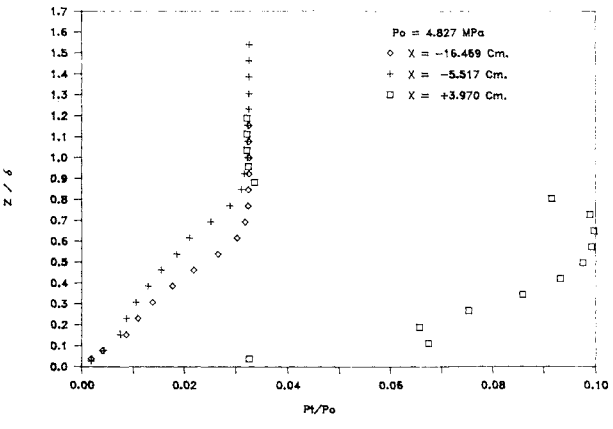

Fig. 2 Nondimensional surface pressure distribution.

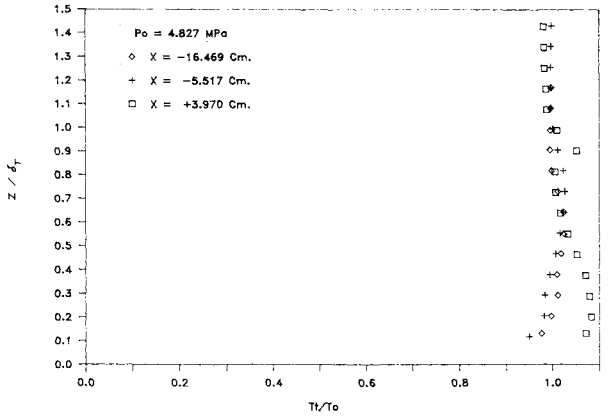

Fig. 3 Nondimensional total temperature ratio at $x = -16.47$ cm, $x = -5.52$ cm, and $x = +3.97$ cm.

Inspection of Fig. 3 clearly indicates the level of overshoot recorded in the total temperature profiles. In general, an 8% overshoot was observed in the total temperature measured on the ramp, as compared to a 3% increase at $x = -5.577$ cm (upstream of the ramp inspection point). This increase in T_t may be a result of the combined viscous and turbulent shear stresses in the outer portion of the boundary layer doing work on the fluid to increase its internal energy, hence, increasing the temperature of the fluid in the inner region of the boundary layer. Also observed was a second temperature maximum in T_t profiles. This second overshoot surpassed T_0 by approximately 3% and appears to be a result of the unsteadiness in the separating shock upstream of the plate/wedge intersection point. Furthermore, the average position of the momentum shear layer (determined from the ramp total pressure profile) only varied by 12%, from the location of this weak second T_t maximum. The first maximum in T_t was located at $Z/\delta_T = 0.22$

Additional support for the multiple T_t peaks were found from measurements obtained on a 24-deg ramp at Mach 2.84 and a unit Reynolds number of 65 × 10^6 by Selig et al.[11] Using hot-wire anemometry, they recorded bimodal mass-flux probability density functions on the ramp, and a single maximum at upstream measurement stations. That is, the mass-flux turbulence intensity profiles acquired on the ramp were determined to have multiple peaks.

The difference between the nondimensional locations (Z/δ_T) of the T_t maximum in the present study to the turbulent intensity profiles of the Selig study was < 30%. This supports the idea and importance of the turbulent stresses locally heating the flow and producing the observed increase in T_t.

References

[1]Holden, M. S., "A Review of Aerothermal Problems Associated with Hypersonic Flight," AIAA 24th Aerospace Sciences Meeting, Reno, NV, AIAA Paper 86-0267, Jan. 1986.

[2]Bogdonoff, S. M., Vas, I. E., Settles, G. S., and Simper, G., "Research on Supersonic Turbulent Separated and Reattached Flows," Aerospace Research Lab., Wright-Patterson AFB, Dayton, OH, Final Rept. ARL 75-0220, June 1975.

[3]Kuehn, D. M., "Turbulent Boundary-Layer Separation Induced by Flares on Cylinders at Zero Angle of Attack, " NASA TR R-117, 1961.

[4]Kuehn, D. M., "Experimental Investigation of the Pressure Rise Required for the Incipient Separation of Turbulent Boundary Layers in Two-Dimensional Supersonic Flow," NASA Memo 1-21-59A, Feb. 1959.

[5]Roshko, A., and Thomke, G. J., "Supersonic, Turbulent Boundary-Layer Interaction with a Compression Corner at Very High Reynolds Number," *Proceedings of Viscous Interaction Phenomena in Supersonic and Hypersonic Flow,* USAF Symposium, Aerospace Research Labs., Dayton, OH, May 1969, p. 109.

[6]Sterrett, J.R., and Emery, J. C., "Experimental Separation Stu-

dies for Two-Dimensional Wedges and Curved Surfaces at Mach Numbers of 4.8 to 6.2," NASA TN D-1014, Feb. 1962.

[7]Todisco, A., and Reeves, B. L., "Turbulent Boundary-Layer Separation and Reattachment at Supersonic and Hypersonic Speeds," *Proceedings of Viscous Interaction Phenomena in Supersonic and Hypersonic Flow,* USAF Symposium, Aerospace Research Labs., Dayton, OH, May 1969, p. 139.

[8]Disimile, P. J., and Scaggs, N. E., "The Effect of Separation on Turbulent Boundary Layer Characteristics Over a Smooth Surface at Mach 6.0," AIAA Paper 90-3028, Portland, OR, Aug. 1990.

[9]Roshko, A., and Thomke, G. J., "Flare-Induced Interaction Lengths in Supersonic, Turbulent Boundary Layers," *AIAA Journal,* Vol. 14, No. 7, 1976, pp. 873-879.

[10]Disimile, P. J., and Scaggs, N. E., "High Reynolds Number Wedge-Induced Separation Lengths at Mach 6," *AIAA Journal,* Vol. 27, No. 12, 1989, pp. 1827-1828.

[11]Selig, M. S., Andreopoulos, J., Muck, K. C., Dussauge, J. P., and Smits, A. J., "Turbulence Structure in a Shock Wave/Turbulent Boundary-Layer Interaction," *AIAA Journal,* Vol. 27, No. 7, 1989, pp. 862-869.

Surface Flow Patterns on an Ogive-Cylinder at Incidence

David Degani,* Murray Tobak,† and G. G. Zilliac‡
NASA Ames Research Center,
Moffett Field, California 94035

I. Introduction

It is well known that the flow about a body of revolution becomes asymmetric with respect to the angle of attack plane at a sufficiently high angle of attack (cf. Refs. 1-7). This asymmetry may be altered by changing the roll angle position of the nose of the body[5,6] or by placing a small asymmetrically disposed disturbance near the apex.[5,7] With further increase in incidence, the steady asymmetric flow becomes unsteady, and as the angle of attack tends toward 90 deg, the flow pattern approaches that of a circular cylinder in crossflow.

Degani and Zilliac[4] have shown experimentally that in addition to the low-frequency von Kármán vortex shedding from the cylinder portion of an ogive-cylinder body at very high incidence, and a high-frequency unsteadiness resulting from a traveling-wave instability of the shear layer, the flow exhibited a midrange frequency unsteadiness as well (with Strouhal number about twice that associated with von Kármán vortex shedding). Although its source has not been identified, this unsteadiness was found to be limited to angles of attack between 50 and 65 deg. The maximum signal level of fluctuations (using a hot-wire anemometer) was found in a volume of about 4D long × 2D high × 2D wide centered above the ogive-cylinder junction. It was suggested in Ref. 4 that this midrange frequency was the result of vortex interaction.

Zillac et al.[5] and other researchers[3,6] have found experimentally that in the range of angles of attack between 50 and 65 deg the flowfield behaves differently than it does at angles of attack both above and below this range when a small change is enforced on the flowfield. When the nose roll angle changed smoothly, the flow above the body changed between two stable positions only. A rational explanation for this behavior of the flowfield was suggested by Tobak et al.[8] with the support of preliminary, unpublished results of the present paper. According to these results, in the range of angles of attack between 50 and 65 deg, foci may exist in the forebody surface flow pattern on the line of primary separation on each side of the body.

It seems clear that the occurrence of a particular regime of flow unsteadiness at angles of attack between 50 and 65 deg and the bistable nature of the flow within this same angle-of-attack range must be linked to the coincident appearance of foci in the surface flow patterns. In view of the potential importance of the phenomenon in completing our understanding of the flow over bodies at incidence, we consider it worthwhile to document the event more fully. This paper contains a complete set of photographs of the surface flow patterns, obtained for angles of attack between 30 and 85 deg, flow conditions at a Reynolds number of 2.6×10^4.

II. Experimental Approach and Results

Measurements were performed in a 38 × 38 cm, low-turbulence wind tunnel at velocities ranging from 12 to 24 m/s. The maximum freestream turbulence level of this facility, as measured by a hot-wire anemometer, is 0.15%. The quality of wind-tunnel flow has been documented more fully in an internal NASA memorandum, available on request to the authors. Although we recognize that freestream turbulence properties might have influenced the shape and extent of the phenomenon to be reported here, we consider it highly unlikely that they could have caused it to appear. Likewise, we consider that other sources of flow unsteadiness and gravitational force effects, which are always present to an undetermined extent in flow-visualization studies, could not have been the cause of the phenomenon to be reported here.

The model configuration consisted of an $L/D = 3.5$ tangent ogive with an $L/D = 12.5$ cylindrical afterbody. The overall length of the model was 35 cm and the diameter of the cylindrical afterbody portion of the model was 2.16 cm. The model was mounted rigidly on a sting support. No boundary-layer trips were used to stabilize the vortex positions or to cause boundary-layer transition. Judging by the position of the lines of separation on the model, we consider the boundary layer to have been laminar. Maximum wind-tunnel model blockage, based on the projected frontal area of the model, was < 5.0% of the cross-sectional area of the test section at 90 deg angle of attack.

Owing to the relatively low freestream velocity and also the inclination of the model, it was necessary to develop a surface flow visualization medium that was less viscous than the standard oil-titanium oxide mixture. After extensive experimentation, a mixture by volume of approximately 5.0% oil-based black paint, 40.0% paint thinner, and 55.0% kerosene was adopted. It was found that, with brush application, a smooth, thin coat could be applied that would flow readily and dry within a few minutes at the freestream velocities of the test.

Experiments were made at a Reynolds number of 2.6×10^4 with angles of attack ranging from 35 to 85 deg. Figures 1 present photographs of oil flow patterns obtained under the previously mentioned conditions. For each angle of attack, three views are shown: left side, top (leeward) side, and right side. Because the paint was highly thinned to allow better capturing of the separation and reattachment lines, the surface pressure gradient was sufficient to blow away the oil on the windward side. Therefore, this view is omitted in Figs. 1. After the completion of each run, the model was taken out of the wind tunnel and the photographs were taken. At each angle of attack, several experiments were carried out resulting in similar surface flow patterns. In all cases, the reference roll angle was kept unchanged. The circumferential angle of the separation line is about 90 deg from the windward ray for all

Received Aug. 23, 1990; revision received Oct. 26, 1990; accepted for publication Dec. 6, 1990.

*Associate Professor, on leave from Technion—Israel Institute of Technology, Faculty of Mechanical Engineering, Haifa, Israel. Associate Fellow AIAA.

†Staff Scientist. Associate Fellow AIAA.

‡Research Scientist.